

# 1 **Divergent neural circuits for proprioceptive and exteroceptive sensing of the *Drosophila* leg**

2  
3 Su-Yee J. Lee<sup>1</sup>, Chris J. Dallmann<sup>1,2</sup>, Andrew Cook<sup>1</sup>, John C. Tuthill<sup>1\*</sup>, Sweta Agrawal<sup>1,3,\*</sup>

4 <sup>1</sup>Department of Physiology and Biophysics, University of Washington, Seattle, WA, USA

5 <sup>2</sup>Department of Neurobiology and Genetics, Julius-Maximilians-University of Würzburg,  
6 Würzburg, Germany

7 <sup>3</sup>School of Neuroscience, Virginia Tech, Blacksburg, VA, USA

8 \*Correspondence: tuthill@uw.edu, sweta@vt.edu

## 9 10 **Abstract**

11 Somatosensory neurons provide the nervous system with information about mechanical forces originating  
12 inside and outside the body. Here, we use connectomics to reconstruct and analyze neural circuits  
13 downstream of the largest somatosensory organ in the *Drosophila* leg, the femoral chordotonal organ  
14 (FeCO). The FeCO has been proposed to support both proprioceptive sensing of the fly's femur-tibia joint  
15 and exteroceptive sensing of substrate vibrations, but it remains unknown which sensory neurons and  
16 central circuits contribute to each of these functions. We found that different subtypes of FeCO sensory  
17 neurons feed into distinct proprioceptive and exteroceptive pathways. Position- and movement-encoding  
18 FeCO neurons connect to local leg motor control circuits in the ventral nerve cord (VNC), indicating a  
19 proprioceptive function. In contrast, signals from the vibration-encoding FeCO neurons are integrated  
20 across legs and transmitted to auditory regions in the brain, indicating an exteroceptive function. Overall,  
21 our analyses reveal the structure of specialized circuits for processing proprioceptive and exteroceptive  
22 signals from the fly leg. They also demonstrate how analyzing patterns of synaptic connectivity can distill  
23 organizing principles from complex sensorimotor circuits.

## 24 25 **Introduction**

26 To coordinate complex behaviors, circuits in the central nervous system (CNS) require continuous  
27 information about the body and the environment. An important source of feedback are somatosensory  
28 neurons, which provide the nervous system with information about mechanical forces acting on an animal's  
29 body<sup>1,2</sup>. Somatosensory neurons are typically described as either exteroceptive, detecting mechanical forces  
30 generated in the external world, or proprioceptive, detecting the position or movement of body parts.  
31 However, because they are embedded within the body, many somatosensory neurons can detect both  
32 externally- and self-generated forces, making it difficult to determine whether specific somatosensory  
33 neurons are exteroceptive, proprioceptive, or both. Recording from primary somatosensory neurons in  
34 behaving animals can resolve the types of mechanical stimuli they encode<sup>3</sup>, but such experiments are  
35 technically difficult and often not feasible. An alternative approach is to map the connectivity of sensory

36 neurons with downstream circuits, which can provide clues to about putative function. For example, some  
37 proprioceptor axons synapse directly onto motor neurons to generate rapid reflexes<sup>4</sup> (**Figure 1A**).  
38 Somatosensory signals can also be integrated with other sensory cues and internal states to inform action  
39 selection in response to external perturbations<sup>5,6</sup>.

40 Mapping the flow of sensory signals into the nervous system has recently become feasible in small  
41 organisms thanks to advances in serial-section electron microscopy (EM) and computational image  
42 segmentation, which enable the reconstruction of whole synaptic wiring diagrams, or connectomes. Some  
43 of the most comprehensive connectomes reconstructed to date include the brain and ventral nerve cord  
44 (VNC) of the adult fruit fly, *Drosophila melanogaster*<sup>7-11</sup>. The fly brain connectomes have already revealed  
45 new insight into the organization and function of sensory organs on the head. For example, mapping the  
46 projections of mechanosensory neurons from the fly's antenna into the brain revealed the organization of  
47 circuits that support song detection, antennal grooming, and escape<sup>12,13</sup>. Volumetric EM datasets of the fly  
48 VNC<sup>8,9</sup>, which is analogous to the vertebrate spinal cord, now make it possible to reconstruct and analyze  
49 the function of somatosensory signals from other parts of the fly's body, including the legs and wings.

50 In this study, we use connectomic analyses of brain and VNC circuits to investigate the largest  
51 somatosensory organ in the *Drosophila* leg, the femoral chordotonal organ (FeCO) (**Figure 1B**). The  
52 *Drosophila* FeCO is comprised of ~150 excitatory (cholinergic) sensory neurons that can be separated into  
53 five functionally and anatomically distinct subtypes: (1) extension- and (2) flexion-encoding claw neurons  
54 encode tibia position, (3) extension- and (4) flexion-encoding hook neurons sense tibia movement, and (5)  
55 club neurons encode bidirectional tibia movement and low-amplitude (<1  $\mu\text{m}$ ), high frequency vibration  
56 (**Figure 1C-D**)<sup>14,15</sup>. The cell bodies and dendrites of the FeCO are located in the femur of each leg and their  
57 axons project into the VNC (**Figure 1B**)<sup>14-17</sup>.

58 The FeCO is typically described as a proprioceptive organ that monitors the movement and position  
59 of the femur-tibia joint<sup>15,18,19</sup>. However, behavioral evidence suggests that the FeCO may also detect  
60 externally-generated substrate vibrations, perhaps to aid in social communication, predator detection, and  
61 courtship<sup>20-23</sup>. It is currently unknown to what degree the five subtypes of FeCO sensory neurons are  
62 specialized to support specific proprioceptive or exteroceptive functions. The club neurons are the only  
63 FeCO subtype that respond to tibia vibration (**Figure 1D**), suggesting that they may support exteroceptive  
64 vibration sensing<sup>14,15</sup>. However, club neurons also respond to larger movements of the tibia like those that  
65 occur during walking, suggesting that they could also be proprioceptive (**Figure 1C**). Intracellular  
66 recordings from second-order neurons have identified distinct pathways for proprioceptive and vibration  
67 sensing, but in some cases also revealed complex pooling of signals from multiple FeCO subtypes<sup>24,25</sup>.

68 Here, we use the FANC<sup>26</sup> and Flywire<sup>7</sup> connectome datasets to reconstruct and analyze neural  
69 circuits downstream of the FeCO of the fly's front left (T1L) leg. We find that position- and movement-  
70 encoding claw and hook neurons are primarily proprioceptive and connect to local circuits within the VNC  
71 for leg motor control. In contrast, vibration-encoding club neurons connect to intersegmental and ascending  
72 circuits that integrate mechanosensory information from the legs, wings, and neck, and relay it to the brain.  
73 Then, by identifying these ascending projections within the brain, we confirm that this leg vibration  
74 information is relayed to auditory circuits downstream of the antenna. We also identify sparse pathways  
75 that mediate interactions between proprioceptive and exteroceptive circuits, revealing how vibration signals  
76 may directly influence motor output. Overall, our analyses suggest that the FeCO supports both  
77 proprioceptive and exteroceptive functions, which are achieved via specialized somatosensory neurons  
78 connected to specialized downstream circuits.

79

## 80 **Results**

### 81 **Reconstruction and identification of FeCO axons in the FANC connectome**

82 Using software for collaborative proofreading and visualization of the segmented FANC EM dataset (see  
83 Methods), we reconstructed the anatomy and synaptic connectivity of roughly half the FeCO axons from  
84 the front left leg (78 total axons, **Figure 1F-I**). We focused our reconstruction efforts on these FeCO axons  
85 because they project to the front left neuromere of the VNC (also referred to as left T1 or T1L), the region  
86 of the *Drosophila* VNC with the most complete information about leg sensorimotor circuits. All of the  
87 motor neurons controlling the muscles of the front left leg and their presynaptic partners have been  
88 previously identified and reconstructed in FANC<sup>26,27</sup>, and prior neurophysiological recordings of FeCO  
89 axons and their downstream targets were made in the same region<sup>14,15,24,25,28,29</sup>. Unfortunately, leg sensory  
90 axons are among the most difficult neurons to reconstruct in the available VNC connectomes, likely due to  
91 rapid cell-death that begins when the legs are separated from the VNC during sample preparation. Although  
92 our dataset is missing some FeCO axons, we found that the number of novel postsynaptic partners decreased  
93 as we added more axons to the dataset (**Figure S1**), suggesting that our reconstruction covers the major  
94 components of the postsynaptic circuitry.

95 The FeCO consists of five functional subtypes that encode tibia position (extension/flexion),  
96 directional movement (extension/flexion), and bidirectional movement/vibration (**Figure 1C-D**)<sup>19</sup>. We  
97 sorted the reconstructed FeCO axons in the connectome into these functional subtypes based on axon  
98 morphology and comparison with light microscopy images (**Figure 1E-G**; see Methods). Based on an X-

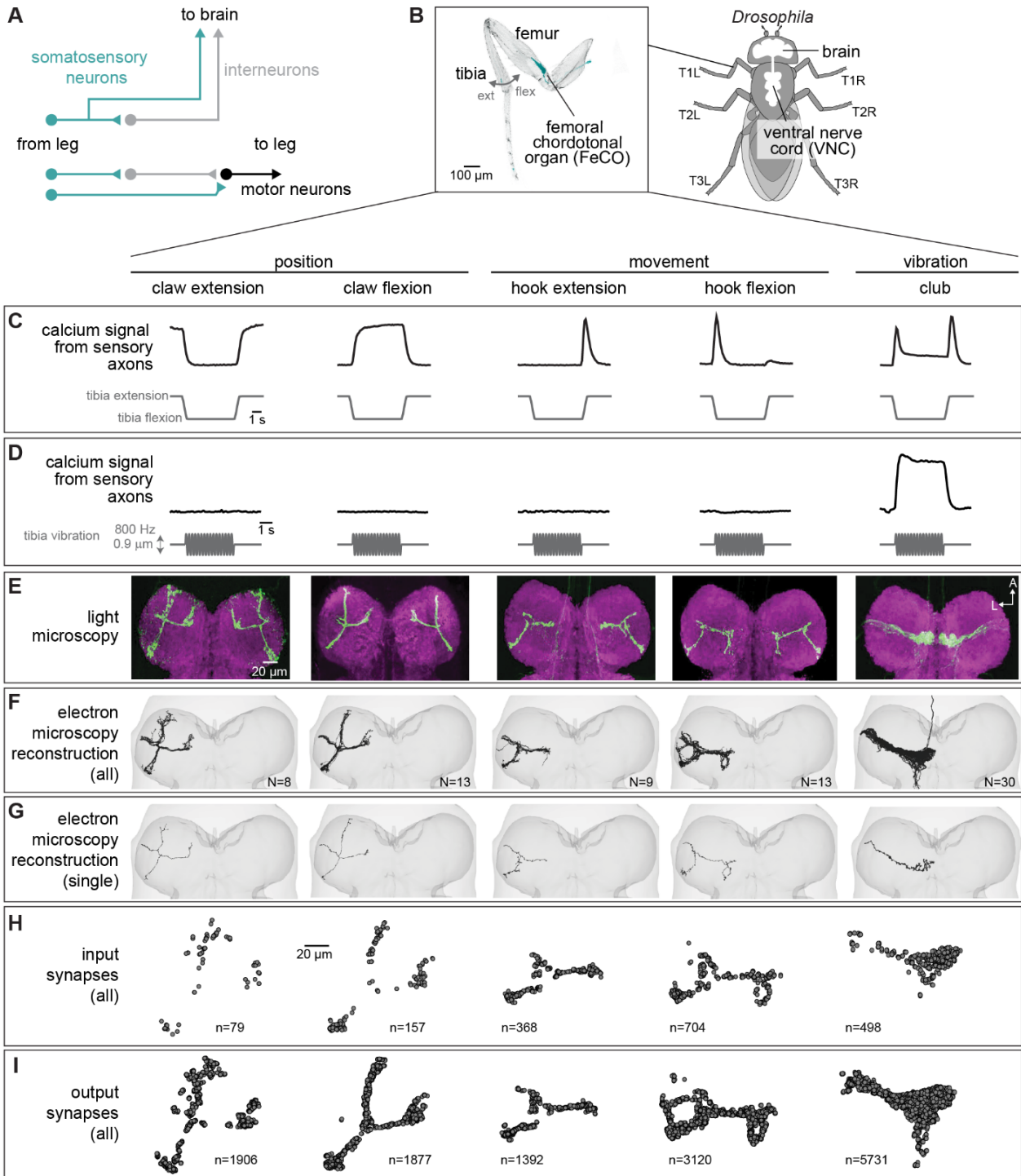


**Figure 1. Connectomic reconstruction of axonal projections from somatosensory neurons in the femoral chordotonal organ (FeCO) of a female *Drosophila*.** (A) Schematic of local and ascending VNC circuits for leg somatosensation and motor control. (B) Left: Confocal image of a *Drosophila* front leg showing the location of FeCO cell bodies and dendrites. Green: GFP; gray: cuticle auto-fluorescence. Right: Schematic showing the fly brain and ventral nerve cord (VNC) (C-I) Anatomical and functional subtypes of somatosensory neurons in the *Drosophila* FeCO. (C) Calcium signals from FeCO axons of each subtype (GCaMP, black traces) in response to a controlled movement of the femur-tibia joint (gray traces). Adapted from Mamiya et al., (2023). (D) Calcium signals from FeCO axons of each subtype (GCaMP, black traces) in response to an 800 Hz vibration of the femur-tibia joint (gray traces). Adapted from Mamiya et al., (2023). (E) Confocal images of the axons of each FeCO subtype in the fly ventral nerve cord (VNC). Green: GFP; magenta: neuropil stain (nc82). Adapted from Agrawal et al., (2020) A: anterior; L: lateral. (F) Reconstructed FeCO axons from each subtype in the front left leg neuromere of the FANC connectome (from left to right, N=8, 13, 9, 13, 35 neurons). (G) Single reconstructed axons from each FeCO subtype in the front left leg neuromere of the FANC connectome. (H) Locations of all input synapses received by each FeCO subtype (i.e. postsynaptic sites). n indicates the number of synapses. (I) Locations of all output synapses made by each FeCO subtype (i.e. presynaptic sites). n indicates the number of synapses.

ray reconstruction of the peripheral cell bodies<sup>14</sup>, we estimate that we reconstructed ~50% of the T1L axons of each subtype: 8 claw extension, 13 claw flexion, and 9 hook extension axons (of ~58 axons), 13 hook flexion axons (of ~28 axons), and 35 club axons (of ~66 axons). Overall, EM reconstructions of axons from each subtype resemble light-level images of FeCO axons<sup>15</sup>, including 5 club axons from the T1L leg that send an ascending projection to the brain. A few FeCO axons, however, demonstrate unexpected within-type diversity, including axons with shortened or doubled branches (**Supplemental Table 1**). As expected for sensory neurons, all FeCO axons have more presynaptic sites (i.e., output synapses) than postsynaptic sites (i.e. input synapses) (**Figure 1H-I**). Generally, the locations of pre- and postsynaptic sites are intermingled; FeCO axons do not have distinct pre- and postsynaptic zones.

109

### 110 **Claw and hook (but not club) axons provide feedback to local leg motor circuits**

111 To investigate pathways downstream of the different FeCO subtypes, we reconstructed the anatomy and synaptic connectivity of all postsynaptic partners that receive at least 4 synapses from a FeCO axon, a threshold used by previous studies<sup>7,30,31</sup>. We classified all postsynaptic VNC neurons into six morphological classes (see Methods): local neurons located entirely in the T1L neuromere: (1) interneurons, (2) motor neurons, (3) sensory neurons, (4) descending and (5) ascending neurons that connect the brain and VNC, and (6) intersegmental neurons, which span multiple VNC neuromeres (**Figure 2A**). We interpret connectivity of FeCO axons with local interneurons or leg motor neurons as suggesting a role in local, rapid feedback control of leg motor output. In contrast, we interpret connectivity with ascending neurons as suggesting a role in mediating sensation and behavior on longer timescales, such as sensory perception and action selection.

121 We found that the majority of synapses from claw and hook extension axons are onto local VNC interneurons and leg motor neurons (**Figure 2B-C**). In contrast, more than half of all synapses from club axons are onto intersegmental neurons. Hook flexion axons are somewhere in between, making roughly similar proportions of their synapses onto local and intersegmental postsynaptic partners. Club and hook flexion axons also make a notably high number of synapses onto ascending neurons that convey leg somatosensory information to the brain.

127 We next used anatomical criteria to identify the developmental origins of all pre- and postsynaptic partners of FeCO axons (see Methods). About 95% of adult neurons in the *Drosophila* VNC arise from 30 segmentally repeated neuroblasts (neural stem cells), each of which divides to form an ‘A’ and ‘B’ hemilineage<sup>32</sup>. Developmental hemilineages are an effective means to classify VNC cell types: neurons of the same hemilineage release the same primary neurotransmitter<sup>33</sup> and express similar transcription

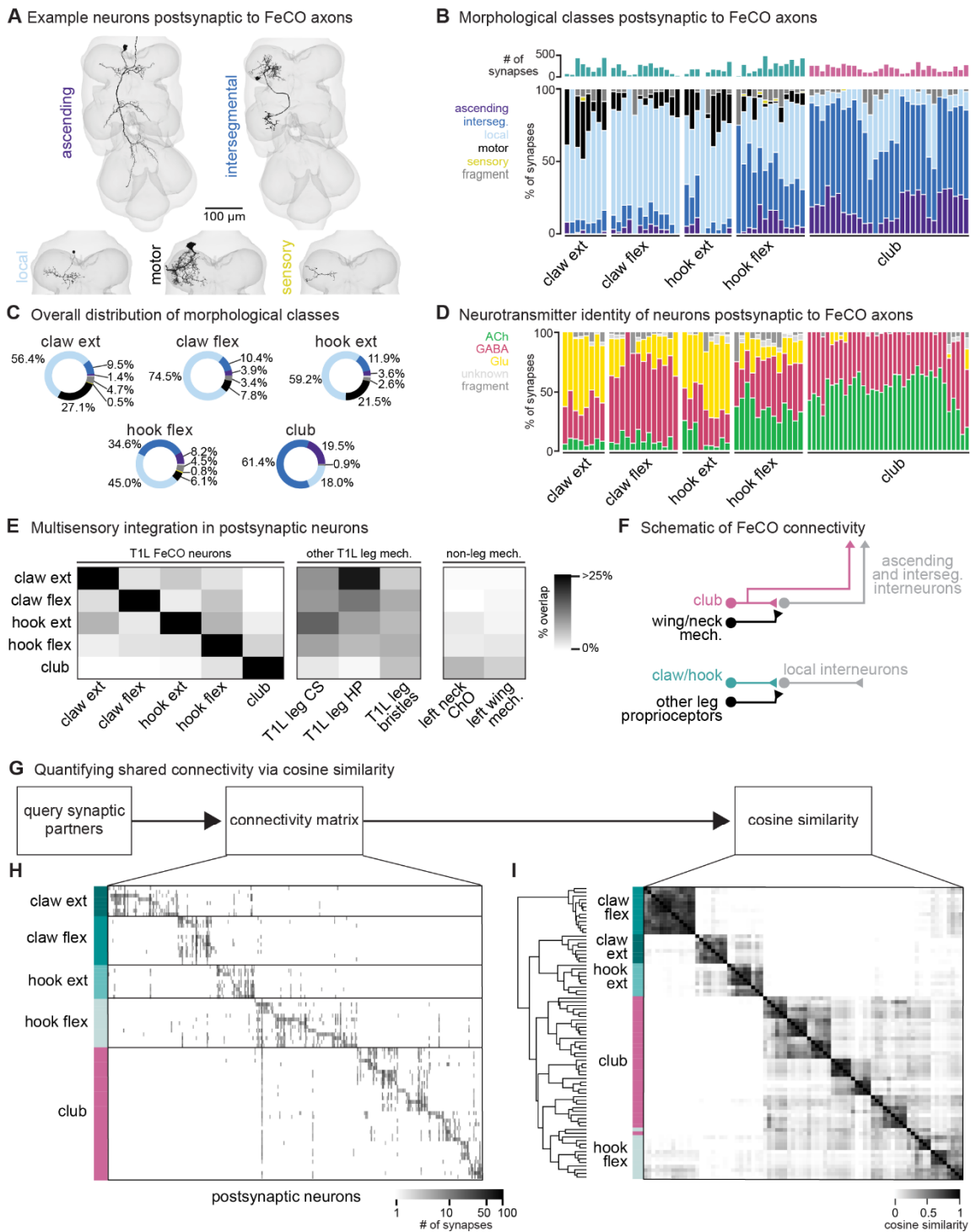


**Figure 2. FeCO neurons exhibit subtype-specific postsynaptic connectivity.** (A) We reconstructed all VNC neurons postsynaptic to FeCO axons from the front left leg (T1L) and classified them into morphological classes. Example provided from each class. (B) Percent of synapses from each FeCO axon that are made onto VNC neurons of each morphological class. Top bar plot shows the total number of output synapses made by each FeCO axon. (C) Per FeCO subtype, the total fraction of output synapses made onto each morphological class. (D) Proportion of total synapses made by each FeCO neuron onto cholinergic (green), glutamatergic (yellow), GABAergic (pink), and unidentified (light gray) hemilineages. (E) Heatmap shows the percent of neurons postsynaptic to a particular T1L FeCO subtype (as indicated along the rows) that also receive synaptic input from an alternate somatosensory population: T1L FeCO neurons, including claw extension axons, claw flexion axons, hook extension axons, hook flexion axons, or club axons, other T1L leg mechanosensory neurons, including campaniform sensilla axons (CS), hairplate axons (HP), or bristle axons, and non-leg mechanosensory neurons, including left neck chordotonal organ axons or left wing somatosensory axons. We found that neurons postsynaptic to claw and hook axons also integrate information from other leg proprioceptors such as HP axons and CS axons. In contrast, neurons postsynaptic to club axons do not integrate information from other leg proprioceptors, but they do integrate information from wing and neck somatosensory axons. (*legend contd. on next page*)

(Fig. 2 legend contd.) (F) Schematic of FeCO connectivity. Club information is conveyed primarily to ascending and intersegmental neurons, who also receive information from wing and neck somatosensory neurons. Information from claw and hook axons is primarily relayed to local interneurons, which also receive information from other leg proprioceptive neurons. (G) By querying the connectivity of each postsynaptic partner of each reconstructed FeCO neuron, we obtained (H) a connectivity matrix and (I) a cosine similarity matrix. (H) Connectivity matrix between FeCO axons and postsynaptic VNC neurons. The shading of each tick indicates the number of synapses from each FeCO axon (row) onto each postsynaptic VNC neuron (column). Colored bars along the left indicate the presynaptic FeCO subtype for that row. FeCO axons are organized by morphological subtype and then by their cosine similarity scores. VNC neurons are organized by their cosine similarity scores. (I) Clustered pairwise cosine similarity matrices of all FeCO axons based on their postsynaptic connectivity. The cosine similarity between two neurons is the dot product of the normalized (unit) column weight vectors. If two FeCO neurons synapse with similar synaptic weights onto the same postsynaptic neuron, relative to the FeCO's total output, the pairwise cosine similarity is 1. FeCO neurons with similar postsynaptic connectivity patterns cluster together, forming connectivity clusters.

133 factors<sup>34,35</sup>. Previous research also suggests that neurons within a hemilineage are functionally related:  
134 thermogenetic activation of single hemilineages drove coordinated movements of legs or wings<sup>36</sup>, and  
135 connectome analyses of larval VNC neurons demonstrated that neurons within a hemilineage share common  
136 synaptic partners<sup>37</sup>.

137 We found that club axons target neurons from different hemilineages than claw and hook axons  
138 (**Figure S2**). Neurons that are primarily postsynaptic to club axons come from hemilineages 8B, 10B, 23B,  
139 0A/0B, 1B, and 9A. Of those, only 1B and 9A neurons receive any synaptic input from claw axons, but the  
140 connectivity is weak (~6.34% and 0.46% of total FeCO input, respectively). Club and hook flexion axons  
141 target some shared hemilineages, including 23B, 1B, and 9A. Neurons from all other identified  
142 hemilineages are predominantly postsynaptic to claw or hook axons and do not receive any synaptic input  
143 from club axons. We further used the hemilineage designations to infer a neuron's likely primary  
144 neurotransmitter (**Figure 2D**). The majority of *Drosophila* neurons release one of three primary  
145 neurotransmitters: acetylcholine, GABA, or glutamate<sup>34,38</sup>. In the fly, acetylcholine is typically excitatory,  
146 while GABA is typically inhibitory<sup>34,39,40</sup>. Glutamate is excitatory at the fly neuromuscular junction, acting  
147 on ionotropic glutamate receptors (GluRs), but is frequently inhibitory in the CNS, acting on the glutamate-  
148 gated chloride channel, GluCl<sup>41</sup>. Club axons synapse onto very few putative glutamatergic neurons (**Figure**  
149 **2D**) compared to claw and hook axons.

150 We conducted similar analyses examining the presynaptic inputs to FeCO axons (**Figure S3**).  
151 Generally, hook axons receive the most input synapses and have the most presynaptic partners, which  
152 include local, ascending, and intersegmental neurons (**Figure S3A-B**). The majority of input synapses to  
153 FeCO axons are GABAergic (**Figure S3D**). The strongest input comes from 9A neurons, which are  
154 primarily presynaptic to hook axons (**Figure S3C-D**). Recent work found that a subset of 9A neurons  
155 suppress expected proprioceptive feedback during voluntary movement such as walking or grooming<sup>29</sup>.

156 Together, these differences in postsynaptic connectivity suggest that claw and hook axons are  
157 connected to postsynaptic partners that are distinct from those downstream of club axons. These  
158 downstream partners differ in their morphology as well as their developmental stem-cell lineage. Hook and

159 claw axon connectivity with local and motor neurons suggests that they play a role in fast feedback control  
160 of leg motor output. In contrast, club axons connect to intersegmental and ascending pathways that could  
161 relay leg vibration information to the brain to support detection of external mechanosensory signals. (**Figure**  
162 **2F**). In support of this conclusion, we found that the neurons that receive input from claw and hook axons  
163 also receive input from other leg proprioceptors, such as hair plate and campaniform sensilla neurons,  
164 whereas the VNC neurons that receive input from club axons receive input from somatosensory neurons on  
165 the neck and wing, not on the leg (**Figure 2E-F**).

166

### 167 **FeCO axons demonstrate subtype-specific downstream connectivity**

168 We next investigated the specific postsynaptic partners targeted by claw, hook, and club axons and  
169 the degree to which FeCO axons synapse onto distinct or overlapping circuits. First, we constructed a  
170 connectivity matrix to look at the postsynaptic connectivity of each FeCO neuron, organizing the rows of  
171 the matrix by FeCO subtype (**Figure 2G-H**). Generally, postsynaptic connectivity is sparse, with each  
172 FeCO neuron contacting only about  $21.1 \pm 1.1$  (mean  $\pm$  s.e.m.) distinct postsynaptic partners. To quantify  
173 this connectivity structure, we calculated the cosine similarity score for pairs of FeCO axons based on their  
174 synaptic outputs (**Figure 2I**; see Methods). Two FeCO axons have a high cosine similarity score if they  
175 make the same relative number of synapses onto the same postsynaptic neurons. Low similarity scores  
176 indicate either that two FeCO axons share few postsynaptic partners or that the relative number of synapses  
177 onto common postsynaptic partners are different.

178 Hierarchical clustering of cosine similarity scores confirmed that FeCO axons of the same subtype  
179 provide similar synaptic output to the same postsynaptic partners (**Figure 2I**). FeCO axons tuned to  
180 different tibia positions (claw flexion vs. claw extension axons) or movement directions (hook flexion vs.  
181 hook extension axons) demonstrate very low (almost zero) cosine similarity scores, indicating that their  
182 postsynaptic connectivity is very different. Instead, hook and claw axons that share directional selectivity  
183 (claw and hook flexion or claw and hook extension axons) demonstrate some shared connectivity, as  
184 suggested by cosine similarity scores above zero. Unexpectedly, we found that hook flexion axons and club  
185 axons share some postsynaptic connectivity, as demonstrated by their relatively high cosine similarity  
186 scores and co-clustering. For example, one specific VNC interneuron received synaptic input from almost  
187 all club and hook flexion axons. We also calculated and clustered the similarity scores for FeCO axons  
188 based on their synaptic inputs (**Figure S3E-F**). However, because FeCO axons have far fewer (and in some  
189 cases zero) presynaptic partners ( $2.9 \pm 0.3$  neurons, mean  $\pm$  s.e.m.), these similarity scores are dominated  
190 by the shared connectivity of just a few presynaptic neurons. Claw extension and claw flexion axons receive  
191 little shared synaptic input. In contrast, hook flexion and hook extension axons all receive very similar



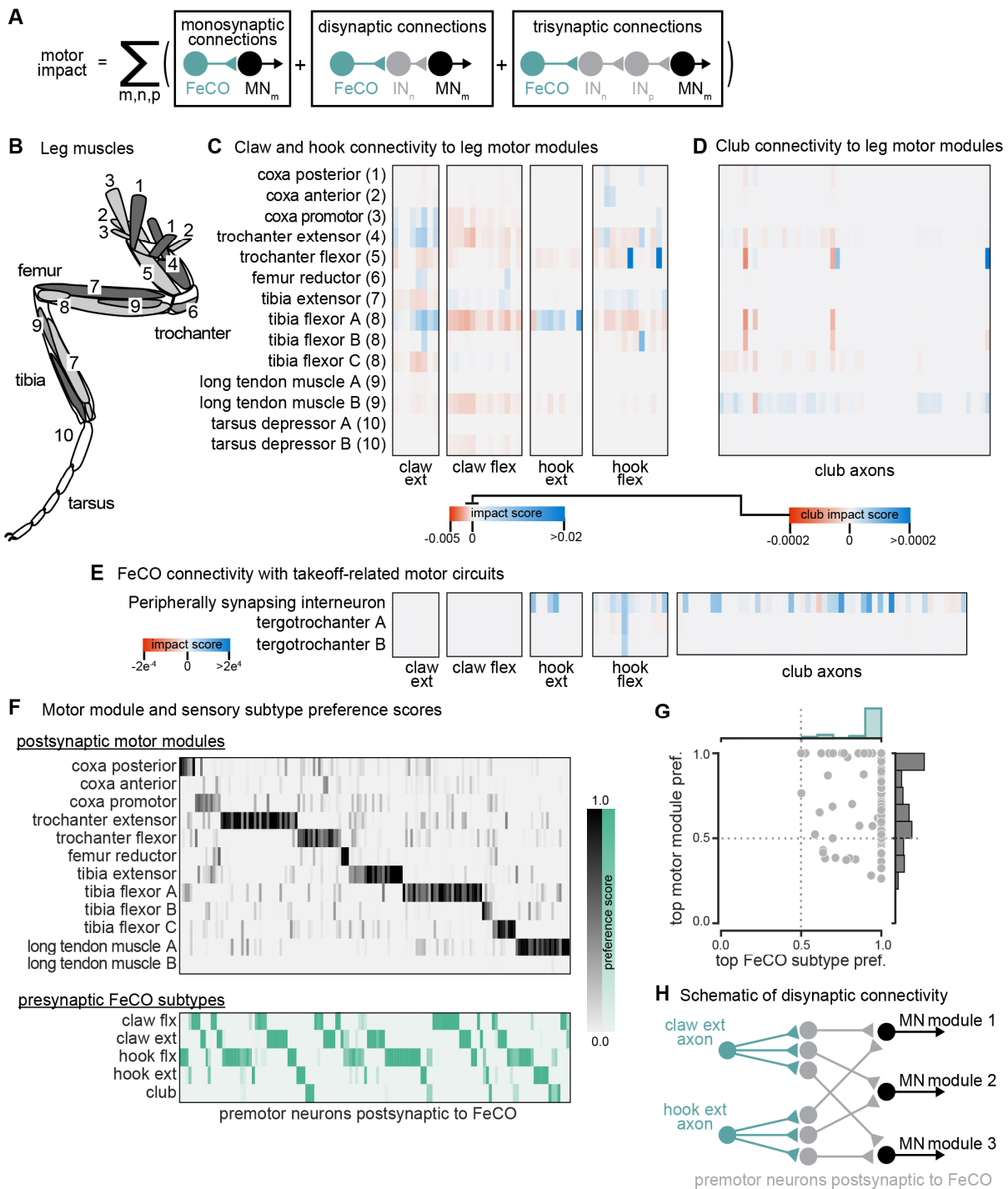


**Figure 3. The connectivity of hook and claw neurons is structured to impact activity of leg motor neurons.** (A) We developed an impact score that takes into account monosynaptic, disynaptic, and trisynaptic connections between FeCO axons and leg motor neurons (see methods). (B) Schematic of the 18 muscles controlling the fly's front leg. Numbers correspond to motor module labels in panel C. (C) Motor impact scores of claw and hook axons on leg motor modules. Motor modules are functional groupings of motor neurons that receive common synaptic input and act on the same joint<sup>27</sup>. The target muscles of each motor module are indicated in panel B. (D) Motor impact scores of club axons on leg motor modules. Note the scale bar change from panel C. (E) Motor impact scores of FeCO axons onto take-off related motor circuits. The peripherally synapsing interneuron is a premotor neuron involved in takeoff. The tergotrochanter is a leg muscle that is not active during walking but is instead involved in jumping and takeoff<sup>26,43,44</sup>. (F) Motor module preference scores (gray, top) and FeCO subtype preference scores (green, bottom) for each premotor VNC neuron that receives input from FeCO axons (columns). Premotor neurons are arranged according to their preferred motor module followed by their preferred FeCO subtype. (G) Motor module preference (y-axis) plotted against FeCO subtype preference (x-axis) for each premotor VNC neuron that receives input from FeCO axons. (H) Schematic representation of the predominant connectivity pattern seen between FeCO neurons and motor modules. Premotor neurons postsynaptic to the FeCO are primarily dedicated to relaying information from a particular FeCO subtype to a particular motor module.

193 synaptic input. Only a small number of club axons receive presynaptic input, but those that do exhibit high  
194 similarity to one another, except for two club axons whose upstream connectivity is more similar to that of  
195 hook axons.

196 In summary, FeCO axons demonstrate subtype-specific pre- and postsynaptic connectivity. FeCO  
197 axons within a subtype are generally more similar in their connectivity than FeCO axons of different  
198 subtypes, suggesting that information from each subtype is conveyed in parallel to different downstream  
199 neurons.

200

### 201 **Claw and hook axons connect directly and indirectly to leg motor neurons**

202 Thus far, we have found that club axons synapse on VNC neurons from different morphological  
203 classes and developmental hemilineages than the claw and hook axons. This segregated connectivity  
204 suggests that signals from club neurons are relayed to distinct downstream circuits with different functions  
205 than claw and hook neurons. Given that club neurons are the only subtype that respond to low amplitude,  
206 high frequency vibration, we hypothesized that this distinct connectivity could reflect an exteroceptive  
207 function of club neurons compared to the proprioceptive function of claw and hook neurons. To explore  
208 this hypothesis, we next examined how each FeCO subtype connects to leg motor circuits.

209 Some FeCO axons synapse directly onto motor neurons, but they also indirectly excite or inhibit  
210 motor neurons via intervening interneurons. We developed an impact score metric (**Figure 3A**) that takes  
211 into account both direct and indirect connections between FeCO axons and motor neurons, as well as the  
212 putative neurotransmitter predicted by hemilineage assignment (see Methods). We then calculated the  
213 motor impact score between each FeCO axon and functional pools of leg motor neurons, called motor  
214 modules<sup>27</sup> (**Figure 3B-C**). Motor modules contain varying numbers of motor neurons that, based on their  
215 presynaptic connectivity patterns, comprise a functional motor pool driving a similar movement (e.g., tibia  
216 extension).

217 Claw and hook neurons make direct and indirect connections with many leg motor neurons (**Figure**  
218 **3C**). The pattern of their connectivity is consistent with previous recordings of motor neuron activity and  
219 optogenetic manipulations in *Drosophila*<sup>24,28</sup>. Claw and hook flexion axons provide strong excitatory  
220 feedback to motor neurons that extend the tibia and inhibitory feedback to motor neurons that flex the tibia.  
221 Claw and hook extension axons provide excitatory feedback to motor neurons that flex the tibia and strong  
222 inhibitory feedback to motor neurons that extend the tibia. Claw extension axons also provide excitatory  
223 feedback to other motor modules, such as the motor neurons that move the coxa forward (coxa promotor)  
224 and extend the trochanter. This connectivity suggests that FeCO feedback supports leg motor synergies that  
225 span multiple leg joints.

226 Consistent with our hypothesis that club neurons do not support local leg motor control, club axon  
227 connectivity with leg motor neurons is weak, demonstrated by a low impact score (**Figure 3D**, note different  
228 scale bar). Club axons form no direct synapses onto leg motor neurons. However, they do indirectly and  
229 weakly connect to leg motor neurons innervating the long tendon muscle (LTM) (**Figure 3D**), which has  
230 been shown to control substrate grip<sup>42</sup>. Club axons also indirectly connect to the premotor peripherally  
231 synapsing interneuron (PSI) (**Figure 3E**), which is associated with control of the wing during takeoff<sup>26,43,44</sup>.  
232 This connectivity suggests a pathway by which activation of club neurons could lead to startle or escape  
233 behaviors, such as freezing and take-off.

234 Finally, we analyzed the overall organization of FeCO axons' premotor connectivity. We found that  
235 all postsynaptic premotor interneurons have a strong preference for a single FeCO sensory subtype and a  
236 single MN module (**Figure 3F-G**). This organization suggests that fly leg motor circuits are organized  
237 according to a "labeled line" structure, with dedicated interneurons connecting a single FeCO subtype with  
238 a single motor module (**Figure 3H**).

239

#### 240 **Club connectivity is consistent with a putative tonotopic map of tibia vibration frequency**

241 We next sought to understand how club neurons are functionally organized by further investigating  
242 their anatomical projection patterns and postsynaptic connectivity. Among the five subtypes, club axons  
243 stood out as having the most variable postsynaptic connectivity patterns. Specifically, club axons separated  
244 into subclusters that were more similar to one another than other club axons (**Figure 2I**). Past recordings of  
245 calcium activity from FeCO neurons in response to vibration of the tibia revealed that club axons are  
246 organized tonotopically<sup>14,15</sup>. We therefore wondered whether the connectivity clusters we found in the VNC  
247 connectome could represent functional groupings of club axons tuned to similar vibration frequencies.

248 In support of this hypothesis, we found that the spatial organization of the connectivity subclusters  
249 of club axons reflects the tonotopy observed in prior experimental recordings. Club axons cluster into 3  
250 groups based on the cosine similarity of their postsynaptic connectivity (**Figure 4A**). These connectivity  
251 clusters spatially tile the dorsal-ventral axis (**Figure 4B**), similar to the tonotopic organization seen in  
252 calcium imaging of club axons in response to tibia vibration (**Figure 4C**)<sup>15</sup>. Accordingly, we hypothesize  
253 that the most ventral populations are sensitive to lower frequency vibrations, whereas the most dorsal  
254 populations (including ascending club axons) are sensitive to higher frequency vibrations. To determine  
255 whether this spatial organization is replicated in other leg neuromeres, we reconstructed 14 club axons from  
256 the middle right leg (right T2). Club axons from this leg also separate into three spatially distinct subclusters  
257 that span the dorsal-ventral axis (**Figure 4A-B**). We also found that VNC neurons postsynaptic to club

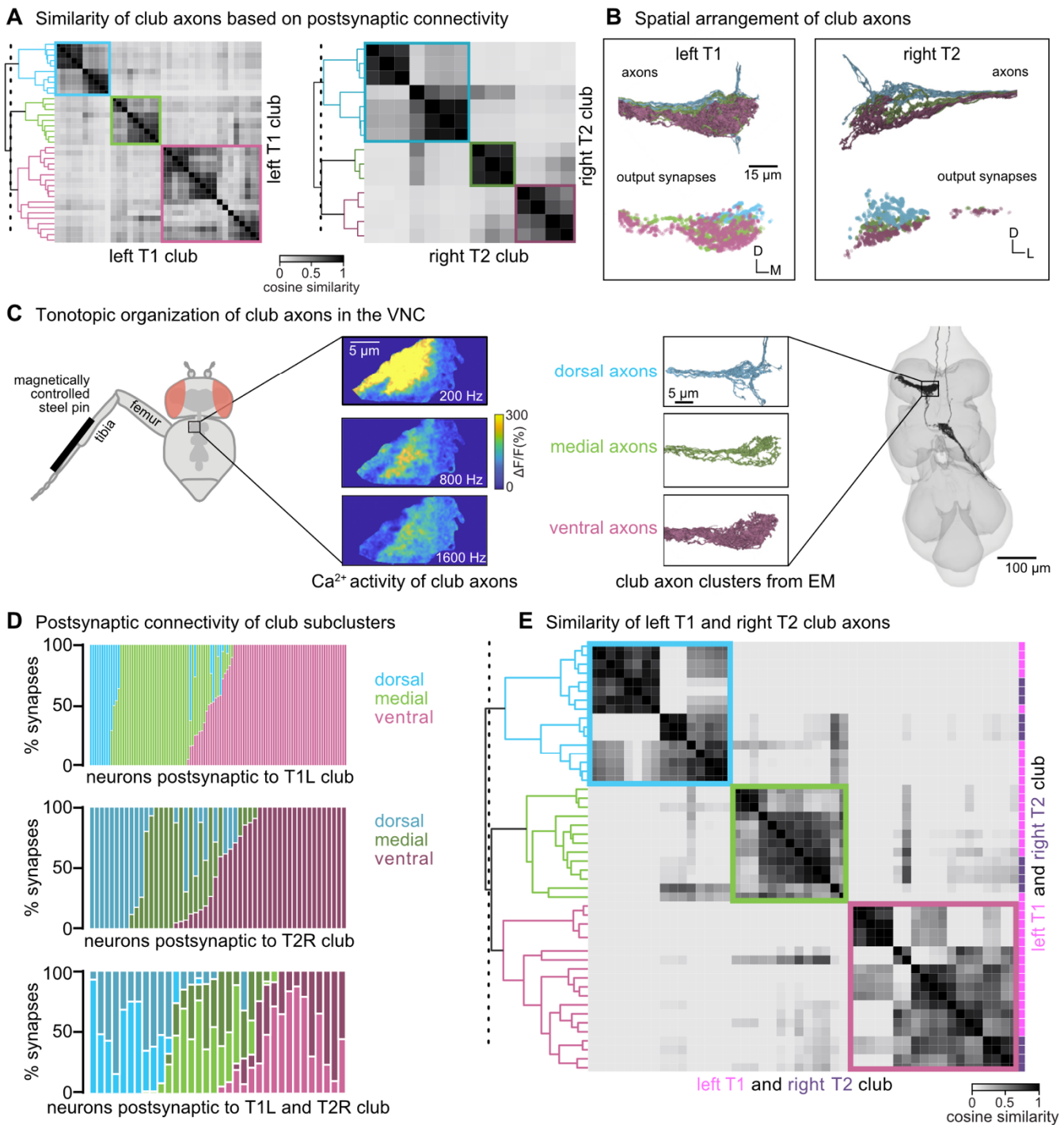


**Figure 4. Club neurons cluster into spatial groups that reflect the putative tonotopic map of tibia vibration frequency.** (A) Clustered pairwise cosine similarity matrices of the club axons based on postsynaptic connectivity. Sensory neurons with similar postsynaptic connectivity patterns cluster together, forming connectivity clusters. Left: Matrices for club axons in front left leg with connectivity clusters highlighted in blue ( $n = 10$ ), green ( $n = 9$ ), pink ( $n = 18$ ). Right: Matrices for club axons in the middle right leg (T2R) with connectivity clusters highlighted in blue ( $n = 7$ ), green ( $n = 3$ ), pink ( $n = 4$ ). (B) Top, Club axons within each connectivity cluster form 3 groups that span the dorsal-ventral axis: dorsal (blue), medial (green), and ventral (pink). Bottom, the spatial location of the output synapses for each of the club neurons color-coded by the corresponding connectivity cluster. (C) The dorsal-ventral organization of connectivity clusters is consistent with tonotopic mapping of tibia vibration frequency recorded from club axons with calcium imaging<sup>15</sup>. Left, Schematic of the experimental set-up. Calcium data from Mamiya et al., (2018) depicting calcium responses from club axons to vibration frequencies (200 Hz, 800 Hz, 1600 Hz) applied to the tibia. Right, reconstructed club axons in the FANC dataset separated by connectivity clusters. (D) Fraction of input synapses from club neurons onto downstream partners. Club neurons are grouped based on connectivity cluster (dorsal: blue, medial: green, ventral: pink). (E) Clustered pairwise similarity matrices of the T1L (pink) and T2R (gray) club axons based on shared postsynaptic connectivity. Sensory neurons with similar postsynaptic connectivity patterns cluster together regardless of their leg of origin.

259 axons receive most of their input from club axons from the same connectivity cluster (dorsal, medial, or  
260 ventral) across multiple legs (**Figure 4D**). Club axons in the most dorsal clusters of the left T1 and right T2  
261 legs connect to overlapping downstream partners regardless of their leg of origin. Similarly, axons in the  
262 ventral-most cluster connect to overlapping downstream partners. Thus, irrespective of the leg of origin,  
263 club axons cluster based on their dorsal-ventral organization (**Figure 4E**).

264 In summary, we found that club axons form subclusters that tile the dorsal-ventral axis and share  
265 postsynaptic partners. We propose that individual club neurons are spatially clustered along the dorsal-  
266 ventral axis based on similarities in vibration frequency tuning. The putative tonotopic structure observed  
267 in club axons is preserved in postsynaptic neurons.

268

### 269 **Interneurons postsynaptic to club axons integrate information across legs**

270 Club axons primarily synapse onto ascending and intersegmental interneurons (**Figure 2**). These  
271 downstream neurons are positioned to integrate vibration information across multiple legs, perhaps to  
272 enable the fly to detect and localize external vibrations (**Figure 5A**). We next investigated the structure of  
273 this putative downstream integration by analyzing the circuitry postsynaptic to club axons. In addition to  
274 reconstructing the interneurons directly downstream of club neurons, we also reconstructed a subset of third  
275 order interneurons.

276 The major downstream partners of club neurons include 8B, 10B, 0A/0B, and 9A neurons (**Figure**  
277 **5B**). These neurons express different primary neurotransmitters – 8B and 10B are cholinergic, whereas  
278 0A/0B and 9A are GABAergic. They also possess distinct morphologies that imply specialized roles in  
279 transforming club information (**Figure 5C-D**). Individual 10B neurons primarily receive input from one leg  
280 and project to the contralateral and adjacent legs, whereas 8B neurons arborize broadly and have mixed  
281 input and output synapses in all six neuromeres. 0A/0B neurons project bilaterally and have pre- and post-  
282 synaptic sites on both the right and left side of each VNC segment. 9A neurons are the most localized, with  
283 their input and output synapses contained within a single neuromere. The diversity of these interneuron  
284 morphologies suggests that club information is broadly relayed across the CNS through parallel pathways  
285 that integrate club information locally within a leg and globally across multiple legs. Integration of club  
286 signals within a leg could be important for amplification while integration across legs could be important  
287 for spatial localization of vibration signals. Lateral and disinhibitory circuits may sculpt vibration  
288 information, for example via normalization or gain control across the population.

289 Additionally, 10B, 8B, 0A/0B, and 9A neurons downstream of club neurons exhibit high levels of  
290 recurrent connectivity among interneurons from different hemilineages and different legs (**Figure 5E**).

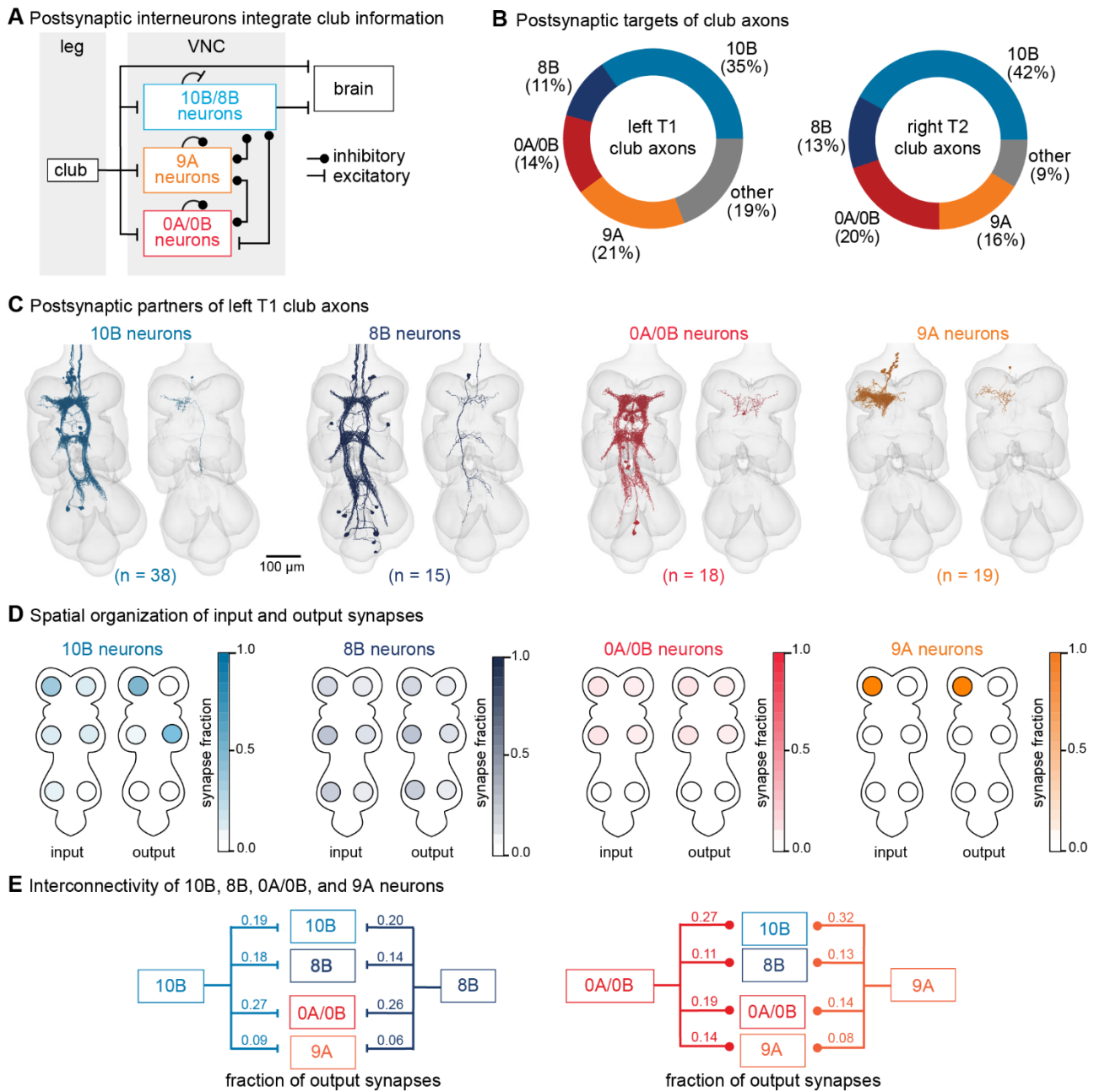


**Figure 5. VNC neurons integrate vibration signals from club neurons across multiple legs.** (A) Schematic of the multi-layered connectivity downstream of club axons. (B) Fraction of total output synapses from club neurons onto downstream interneurons separated by hemilineage class. 10B (light blue,  $n = 38$ ), 8B (dark blue,  $n = 15$ ), 0A/0B (red,  $n = 18$ ), 9A (orange,  $n = 19$ ) (C) Reconstructed interneurons downstream of left T1 club neurons from the FANC dataset. Left image shows all reconstructed neurons of a given hemilineage that are downstream of TIL club neurons. Right image shows a single example neuron from that hemilineage. (D) Heatmap depicting the spatial locations of input (left) and output (right) synapses for 10B, 8B, 0A/0B, and 9A interneurons that are downstream of TIL club neurons. (E) Circuit diagram depicting recurrent connections between 10B, 8B, 0A/0B, and 9A interneurons. Each line indicates an excitatory or inhibitory connection and is labeled with the fraction of total output synapses each interneuron class makes with another interneuron class.

291 Overall, the circuitry downstream of club axons is complex, interconnected, and multi-layered. We  
 292 hypothesize that this highly interconnected circuit architecture supports the fly's capacity to localize  
 293 substrate vibrations in the external environment.  
 294

## 295 **Leg vibration information integrates with auditory circuits in the brain**

296 Vibration signals from club neurons are relayed to the brain by ascending club sensory axons and  
297 ascending 8B and 10B neurons (**Figure 6A**). Since the FeCO has been implicated in sensing substrate  
298 vibrations for courtship and escape, we hypothesized that leg vibration information carried by the ascending  
299 projections is integrated in the brain with other sensory information from the antennae. The fly antenna also  
300 contains a chordotonal organ known as the Johnston's Organ, which detects antennal displacements and  
301 local air vibrations<sup>45-47</sup>. To this end, we next identified where these ascending neurons project to in the  
302 brain and analyzed their downstream connectivity.

303 Within the FANC connectome, we reconstructed 8 ascending club axons from two legs, 58  
304 ascending 10B neurons, and 52 ascending 8B neurons (**Figure 6A**, bottom). We then used a connectome of  
305 the fly brain<sup>7,31</sup> to identify ascending projections that matched light-level morphology of ascending  
306 projections from club axons, 8B neurons, and 10B neurons (**Figure 6A**, top). Within the brain connectome,  
307 we found 24 axons that matched the projections of ascending club axons and 94 axons that matched the  
308 ascending projections of 8B and 10B neurons. Due to the similarity of their ascending projections, we could  
309 not resolve which interneuron axons belonged to which hemilineage (8B or 10B) in the brain connectome.  
310 However, 8B/10B branching patterns in the brain are notably different from those of ascending club  
311 neurons. Club axons are smooth with few branches, while 10B/8B axons branch extensively.

312 To understand how the information in these two ascending pathways differs, we compared their  
313 connectivity in the VNC and the brain (**Figure 6B**). Ascending club axons and 8B/10B neurons are  
314 interconnected and share several downstream partners in the VNC. Approximately 30% of output synapses  
315 from the ascending club axons are onto ascending 8B/10B interneurons. Additionally, the majority of  
316 postsynaptic partners of ascending club axons in the VNC and the brain also receive input from ascending  
317 8B/10B interneurons (**Figure 6B**). However, 8B/10B neurons have many more postsynaptic partners than  
318 club neurons. Thus, 8B/10B neurons target many of the same postsynaptic partners as ascending clubs, but  
319 also contact several non-overlapping downstream partners as well.

320 Consistent with our hypothesis that club neurons are exteroceptive, we found that ascending club  
321 and 8B/10B neurons target known auditory brain regions: the anterior ventrolateral protocerebrum (AVLP),  
322 wedge (WED), saddle (SAD), and gnathal ganglion (GNG) (**Figure 6C-D**). The AVLP, WED, SAD, and  
323 GNG receive integrated auditory information<sup>48</sup> and are responsive to courtship song<sup>49</sup>. Neurons in the WED  
324 also respond to antennal vibrations and are tonotopically organized<sup>45</sup>. Across sensory modalities, the  
325 ascending club and 8B/10B neurons converge onto shared downstream partners with antennal  
326 mechanosensory neurons, namely Johnston's Organ neurons (JONs) (**Figure 6E**). This shared connectivity  
327 suggests that, in the brain, leg vibration information is compared to mechanosensory information from the

328 antennae. We speculate that this comparison could contribute to the detection and localization of mechanical  
 329 vibrations in the external environment (**Figure 6F**).  
 330

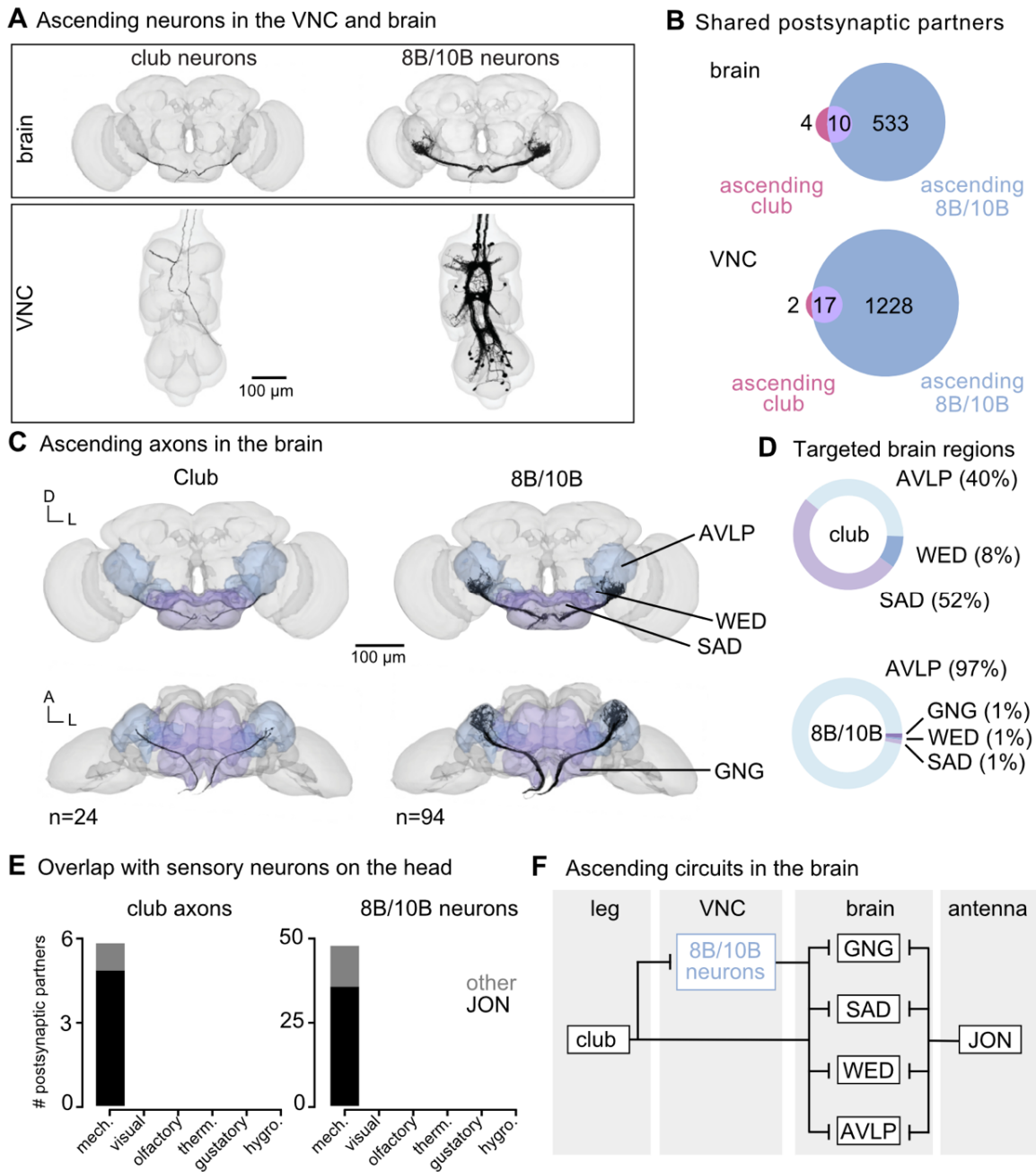


**Figure 6. Vibration signals from club neurons are transmitted directly and indirectly to the brain and integrated with auditory signals from the antenna.** (A) Ascending club axons and ascending 8B and 10B interneurons that are reconstructed in the FANC (bottom, 8 club axons and 52 interneurons) and Flywire (top, 24 sensory axons and 94 interneuron axons) datasets. (B) Venn diagrams of shared postsynaptic partners between ascending club neurons and ascending 8B/10B neurons in the VNC (top) and brain (bottom). (C) Images of the ascending club axons ( $n = 24$ ) and ascending 8B and 10B interneurons ( $n = 94$ ) in the brain dataset with targeted brain regions highlighted (Flywire). Axons project to the anterior ventrolateral protocerebrum (AVLP), wedge (WED), saddle (SAD), and gnathal ganglion (GNG). (D) Percentage of synaptic outputs from ascending club axons (top) and ascending 8B/10Bs interneurons (bottom) in each brain region. The ascending club axons and ascending interneurons differ with respect to distribution of output synapse location. (E) Number of postsynaptic partners of ascending club axons (left) and ascending 8Bs/10Bs (right) that are shared with other sensory neurons in the brain. JON = Johnston's Organ. (F) Circuit diagram depicting the projection patterns of ascending club and ascending 8B/10B interneurons in the brain which integrate with antennal auditory circuits.



## 332 Discussion

333 Here, we use connectomic reconstruction of neural circuits to infer the function of limb  
334 somatosensory neurons from patterns of synaptic connectivity. Our analyses suggest a dual function for the  
335 *Drosophila* femoral chordotonal organ (FeCO): position and movement-sensing claw and hook neurons are  
336 primarily proprioceptive, providing feedback to local leg motor circuits. In contrast, vibration-sensing club  
337 neurons are primarily exteroceptive and provide feedback to intersegmental circuits that integrate  
338 somatosensory information across multiple limbs and then convey that information to the brain. Prior  
339 experiments in *Drosophila* and other insects had suggested a dual function<sup>15,18–23</sup>, but it was previously  
340 unknown whether proprioception and exteroception were supported by distinct or overlapping subtypes of  
341 FeCO sensory neurons and downstream interneurons. These analyses demonstrate the power of  
342 connectomic mapping and analysis to identify putative functions of somatosensory neurons. They also  
343 motivate future work that tests the function of circuits for limb proprioception and exteroception in behaving  
344 flies.

345

### 346 Role of the FeCO in local leg motor control

347 We found that movement- and position-sensing hook and claw axons synapse directly and indirectly  
348 onto leg motor neurons (**Figure 3**). For example, extension-sensitive claw and hook axons provide  
349 excitatory input to the tibia and tarsus flexor motor neurons and inhibitory input to tibia extensor motor  
350 neurons. Flexion-sensitive claw and hook axons demonstrate the opposite pattern of connectivity, primarily  
351 exciting extensors and inhibiting flexors. This connectivity is consistent with prior evidence that the FeCO  
352 contributes to stabilization of leg posture<sup>18,24,28</sup>. Claw and hook axons also provide feedback to motor  
353 neurons controlling movement about other joints. Multi-joint, intra-leg feedback from the FeCO has also  
354 been found in locusts<sup>50</sup> and wētās<sup>51</sup>.

355 Proprioceptive feedback needs to be flexibly tuned to reflect behavioral demands<sup>52</sup>. For example,  
356 during voluntary movement, proprioceptive pathways promoting stabilizing reflexes may be attenuated to  
357 avoid opposing the intended movement. One possible mechanism underlying this context-dependent tuning  
358 is presynaptic inhibition of sensory axons<sup>53,54</sup>. In support of this mechanism, we found several inhibitory  
359 upstream partners of claw and hook axons (**Figure S3**). We also showed in a recent study that hook axons  
360 are presynaptically inhibited during voluntary movement<sup>29</sup>. In addition to direct feedback onto  
361 somatosensory axons, proprioceptive feedback is also likely tuned via context-dependent inhibition of  
362 downstream pathways.

363 Finally, we found that claw and hook axons synapse onto a small number of intersegmental and  
364 ascending neurons (**Figure 2**). Intersegmental projections could relay proprioceptive information to the

365 motor circuits of other legs. However, past work suggests that feedback from the FeCO of one leg does not  
366 strongly affect control of other legs – manipulating activity of FeCO neurons has little effect on inter-leg  
367 coordination<sup>55-57</sup>. One study described intersegmental neural pathways that receive input from the FeCO  
368 and mediate reflexes of adjacent legs, though they did not specifically test the effects of manipulating FeCO  
369 activity<sup>58</sup>. Ascending neurons that are postsynaptic to claw and hook neurons could relay leg proprioceptive  
370 information to the brain to inform motor planning. Calcium imaging experiments have shown that many  
371 ascending neurons are active during behaviors like walking<sup>59</sup>. Additionally, visual neurons and neurons  
372 within motor planning regions of the fly brain, such as the central complex, encode walking stride, speed,  
373 and turning behavior even in the absence of visual input, suggesting that they receive self-motion cues from  
374 the legs<sup>60-62</sup>.

375

### 376 **Tonotopic organization of club axons**

377 Individual club neurons are tuned to specific vibration frequencies, collectively forming a tonotopic  
378 map in the VNC<sup>19,63</sup>. We found that club axons are spatially organized into sub-clusters with shared  
379 postsynaptic connectivity that tile the dorsal-ventral axis of the VNC (**Figure 4**). By comparing this spatial  
380 organization to prior recordings of club axon activity in the VNC<sup>63</sup>, we hypothesize that the most dorsal  
381 club axons respond to higher frequencies while the most ventral club axons respond to lower frequencies.  
382 While all club neurons synapse onto ascending interneurons, only the most dorsal club axons ascend directly  
383 to the brain. Thus, we predict two pathways for club information to reach the brain: 1) a direct sensory  
384 pathway that carries high-frequency vibrations from the legs and 2) an indirect pathway that carries  
385 tonotopically organized and spatially localized vibration information. High-frequency information may be  
386 particularly salient, necessitating a more rapid behavioral response compared to broadband vibrations.  
387 Vibration sensing is an important yet understudied sensory modality in insects and other animals<sup>64</sup>. For  
388 example, recent evidence from mice shows that auditory and high-frequency tactile vibration signals  
389 converge in the inferior colliculus and are used to avoid mechanically vibrating environments<sup>65</sup>.

390

### 391 **Putative exteroceptive function of club neurons**

392 Our analysis of the connectome supports the hypothesis that club neurons primarily function as  
393 vibration-sensing exteroceptors. Insects utilize substrate vibrations for social communication, predator  
394 detection, and environmental sensing, such as wind<sup>66</sup>. Many insect species possess subgenual organs,  
395 specialized vibration sensors in the tibia, but flies and beetles lack these sensory structures<sup>66</sup>. Thus, club  
396 neurons may be the primary sensors for detecting substrate vibrations in the fly leg. Previous studies across  
397 multiple insect species have implicated the FeCO in escape and courtship responses<sup>20,22,23</sup>. Crustaceans also

398 have leg chordotonal organs that can detect both joint movement and external substrate vibrations, with  
399 reported involvement in detecting vibration-based social communications<sup>67-69</sup>.

400 In *Drosophila*, courtship song involves both airborne and substrate-borne vibrations. Males vibrate  
401 their wings, producing an airborne “song” that is detected by females via the antennae<sup>70-73</sup>. Males also tap  
402 their abdomens, producing substrate-borne vibrations that promote pausing in females<sup>74</sup>. Genetic silencing  
403 of FeCO neurons in female flies reduces their receptivity to male courtship song<sup>22</sup>, suggesting that the FeCO  
404 is involved in courtship. Consistent with this hypothesis, we found downstream neurons in the brain that  
405 integrate vibration information from both legs and antennae (**Figure 6**). Vibration-sensitive JONs and club  
406 neurons respond to overlapping vibration frequency ranges applied to the antenna or leg, respectively<sup>19,45-</sup>  
407 <sup>47,63</sup>, but the full sensitivity range for each group has not been carefully measured. We hypothesize that the  
408 integration of vibration information from the antennae and legs could inform courtship behavior by  
409 providing overlapping information regarding both airborne and substrate-borne courtship communication.  
410 Importantly, in this study, we reconstructed the FeCO circuits within a female VNC. If club neurons are  
411 involved in detecting courtship-related signals, the circuitry downstream of the club neurons could be  
412 sexually dimorphic and thus different in male flies.

413 Aside from courtship, vibration information from club neurons could be used for detecting  
414 movements of predators or other threats, such as wind or rain. Consistent with this hypothesis, we found  
415 that club axons are indirectly connected to escape-related neurons, namely the motor neurons innervating  
416 the long tendon muscle (LTM) and the premotor peripherally synapsing interneuron (PSI) (**Figure 3**).  
417 Activation of club neurons could promote leg freezing via activation of the LTM, or take-off via activation  
418 of the PSI.

419

#### 420 **Lack of convergence across FeCO subtypes in second-order neurons**

421 We were surprised to find that the downstream connectivity of each FeCO subtype is quite distinct:  
422 very few VNC neurons receive synapses from more than one FeCO subtype (**Figure 2**). Past work had  
423 proposed a higher degree of convergence across FeCO subtypes. Using whole cell patch-clamp recordings  
424 and 2-photon calcium imaging, one study found multiple VNC interneuron cell types that encode  
425 combinations of femur-tibia joint movement, position, and vibration, suggesting that they receive input  
426 from multiple FeCO subtypes<sup>24</sup>. Another combined optogenetic activation and calcium imaging to directly  
427 map the functional connectivity between FeCO axons and their downstream partners<sup>25</sup>. That study also  
428 found examples of VNC interneurons that receive inputs from more than one FeCO subtype. One possible  
429 explanation for this discrepancy is that our connectomic analyses predominantly focused on direct  
430 connections between FeCO neurons and their synaptic partners. The integration of information from

431 multiple FeCO subtypes could be via indirect connections involving multiple intervening interneurons. In  
432 addition, Agrawal et al., (2020) found strong evidence for gap junctions that connect FeCO sensory neurons  
433 with some downstream partners. The FANC EM dataset was not imaged at sufficient spatial resolution to  
434 resolve electrical synapses. Finally, we did find some weak shared connectivity between FeCO cell types  
435 that share directional selectivity, such as claw and hook flexion axons or claw and hook extension axons.  
436 Due to the adventitious nature of their physiology experiments, Agrawal et al., (2020) and Chen et al.,  
437 (2021) may have, by chance, characterized the few interneurons that do indeed receive synaptic information  
438 from multiple FeCO subtypes.

439 We did find, however, substantial overlap in the downstream connectivity of FeCO neurons and  
440 other leg proprioceptive neurons, such as campaniform sensilla (CS) and hairplates (HP) (**Figure 2E**). In  
441 fact, claw and hook axons shared a larger number of downstream partners with CS or HP neurons than with  
442 other FeCO subtypes. Work from stick insects and other models suggest that such multimodal input is  
443 important for context-dependent control of proprioceptive reflexes<sup>75,76</sup>. For example, signals from load-  
444 sensing CS neurons can reduce the effect of FeCO activation on leg motor neurons.

445 Although there is no overlap in the downstream connectivity of claw axons or hook extension axons  
446 and club axons, we did find some overlap in the connectivity of hook flexion and club axons (**Figure 2**). In  
447 fact, some club axons share more downstream connectivity with hook flexion axons than with other club  
448 axons. This finding is consistent with Agrawal et al., (2020), who found one cell type, 9Aa neurons, that  
449 respond to both flexion and vibration of the femur-tibia joint. However, the implications of this overlap  
450 remain to be investigated. For example, such overlap could enable the fly to determine if the source of the  
451 vibration is due to movement of its leg. Alternatively, perhaps flies concurrently sense movement and  
452 vibration information from the leg to assess substrate texture.

453

## 454 **Looking forward**

455 Connectome analysis is a powerful tool to generate and falsify hypotheses about circuit function.  
456 Thanks to advances in serial-section electron microscopy and image segmentation, we are close to having  
457 multiple connectomes of small model organisms. As more neurons within these connectomes are connected  
458 to specific functions, such as motor neurons that control a particular joint or sensory neurons that detect  
459 specific signals, these maps become increasingly useful anatomical frameworks for generating hypotheses  
460 about the neural control of behavior. Though physiological and behavioral measurements are still necessary  
461 in order to determine how a circuit functions, our study illustrates how a global view of synaptic  
462 connectivity can reveal organizing principles that motivate future experiments.

463

464 **Acknowledgements**

465 We thank members of the Tuthill laboratory for technical assistance and feedback on the manuscript. We  
466 also thank Jasper S. Phelps, Wei-Chung Allen Lee, and the FANC community for their contributions to the  
467 proofreading of the VNC connectome. We thank Leila Elabaddy, Ellen Lesser, Shirin Mohammadian,  
468 Gwendolyn Swannell, and Brandon Pratt for granting us permission to use their unpublished reconstructions  
469 of sensory neurons in FANC. We thank Jim Truman, David Shepherd, Haluk Lacin, and Elizabeth Marin  
470 for assistance with hemilineage identification. This work was supported by a Postdoctoral Research  
471 Fellowship from the Deutsche Forschungsgemeinschaft (DFG, German Research Foundation) project  
472 432196121 to C.J.D, a Searle Scholar Award, a Klingenstein-Simons Fellowship, a Pew Biomedical  
473 Scholar Award, a McKnight Scholar Award, a Sloan Research Fellowship, the New York Stem Cell  
474 Foundation, and NIH grants R01NS102333 and U19NS104655 to J.C.T., NIH grants K99NS117657 and  
475 R00NS117657 to S.A, and NIH grant T32 NS 99578-3 to S.J.L. and J.C.T.

476

477 **Methods**

478

479 **Key resources table**

Reagent type (species) or resource	Designation	Source or reference	Identifiers	Additional information
Deposited data	FANC connectome	Azevedo et al. (2022)	<a href="https://fanc.community">https://fanc.community</a>	
Deposited data	FAFB/FlyWire connectome	Dorkenwald et al. (2023), Schlegel et al. (2023)	<a href="https://flywire.ai">https://flywire.ai</a>	
Software, algorithm	CAVEclient	Dorkenwald et al. (2023)	<a href="https://github.com/seunglab/CAVEclient">https://github.com/seunglab/CAVEclient</a>	
Software,	neuPrint	Plaza et al.	<a href="https://neuprint.jan">https://neuprint.jan</a>	

algorithm		(2022)	elia.org/	
Software, algorithm	Neuroglancer		RRID:SCR_01563 1	
Software, algorithm	Python		RRID:SCR_00839 4	

480

481 **Reconstruction of neurons in the FANC connectome**

482 Neurons in the Female Adult Nerve Cord (FANC) electron microscopy dataset<sup>8</sup> were previously segmented  
 483 in an automated manner<sup>26</sup>. To manually correct the automated segmentation of our neurons of interest, we  
 484 used Google’s collaborative Neuroglancer interface<sup>77</sup>. Many of the FeCO axons in T1L were previously  
 485 identified<sup>8</sup>, and most of the claw and hook axons were previously corrected<sup>29</sup>. Here, we identified and  
 486 corrected additional claw axons as well as all club axons in T1L and T3R. Identification was guided by  
 487 light-level images of FeCO subtype-specific genetic driver lines<sup>15,19</sup>.

488 To reconstruct pre- and postsynaptic partners of FeCO neurons, we identified all objects in the  
 489 automated segmentation that received at least 4 synapses from an FeCO neuron or made at least 3 synapses  
 490 onto an FeCO neuron. We then proofread those objects until associated with either a cell body, or an  
 491 identified descending or sensory process. A small number of objects were categorized as fragment segments  
 492 and could not be connected to a cell body or an identified descending or sensory process. We deemed a  
 493 neuron as “proofread” once its cell body was attached, its full backbone reconstructed, and as many  
 494 branches as could be confidently attached. Neuron annotations were managed by CAVE, the Connectome  
 495 Annotation Versioning Engine<sup>78</sup>. We used custom Python scripts to interact with CAVE via CAVEclient<sup>78</sup>.

496

497 **Novel partners analysis**

498 To identify the number of new postsynaptic partners added to our dataset per each FeCO sensory neuron  
 499 we reconstructed, we first found all postsynaptic partners of all reconstructed T1L FeCO axons. Then, we  
 500 randomly sampled the FeCO neurons one at a time (without replacement) in a cumulative fashion, and  
 501 calculated how many novel postsynaptic partners were connected to each additional FeCO neuron. We re-  
 502 did this random sampling fifty times.

503

504 **Cosine similarity scores**

505 Cosine similarity (for example, **Figure 2I**) was calculated using the cosine similarity method from the  
506 scikit-learn python package. Cosine similarity scores were then hierarchically clustered using the  
507 agglomerative clustering methods from the scikit-learn python package.

508

### 509 **Definition of cell classes**

510 Neurons pre- and postsynaptic of FeCO axons were identified as motor, sensory, ascending, descending,  
511 intersegmental, or local neurons. Motor neurons have a cell body in the VNC and a process in the leg nerve.  
512 These neurons were recently identified in the FANC dataset for the front left leg<sup>26,27</sup>. Sensory neurons have  
513 a process in the leg nerve but no cell body in the VNC. Ascending neurons have a process in the neck  
514 connective and a cell body in the VNC. Descending neurons have a process in the neck connective but no  
515 cell body in the VNC. Intersegmental and local neurons have a cell body and all processes in the VNC. The  
516 processes of intersegmental neurons spanned multiple neuromeres, whereas those of local neurons were  
517 contained in a single neuromere. All pre- and postsynaptic neurons were manually checked to make sure  
518 they were in the correct categories.

519

### 520 **Identification of hemilineages**

521 In *Drosophila*, neurons that share a developmental origin (i.e., belong to the same hemilineage) possess  
522 common anatomical features<sup>36</sup> and release the same fast-acting neurotransmitter (e.g. GABA, glutamate, or  
523 acetylcholine)<sup>33</sup>. We took advantage of this knowledge to identify the hemilineage of each neuron upstream  
524 and downstream of FeCO axons in the FANC connectome. We first identified and grouped together local,  
525 intersegmental, and ascending VNC neurons based on where their primary neurite entered into the neuropil.  
526 These groups of similar primary neurites were then identified as known hemilineages using light  
527 microscopy images of sparse GAL4 lines, cell body position along the dorsal-ventral axis<sup>33,36,79,80</sup>, and  
528 personal communication (James W. Truman, David Shepherd, Haluk Lacin, and Elizabeth Marin). Putative  
529 neurotransmitter was then assigned by referencing Lacin et al., (2019). Not all of the clues are available for  
530 all of the neurite bundles. See **Supplemental Table 2** for links to view entire populations of each  
531 hemilineage in Neuroglancer, an online tool for viewing connectomics datasets<sup>77</sup>.

532

### 533 **Motor impact score**

534 A presynaptic neuron's monosynaptic impact score onto a postsynaptic neuron is defined as the number of  
535 synapses made by the presynaptic neuron onto the postsynaptic neuron, divided by the total number of input  
536 synapses received by the postsynaptic neuron. Then, based on the presynaptic neurons' putative  
537 neurotransmitter according to its hemilineage assignment, this impact score is either considered excitatory

538 (or positive) or inhibitory (or negative). In the fly, acetylcholine is typically excitatory, while GABA is  
539 typically inhibitory<sup>34,39,40</sup>. Glutamate is excitatory at the fly neuromuscular junction, acting on ionotropic  
540 glutamate receptors (GluRs), but is frequently inhibitory in the CNS, acting on the glutamate-gated chloride  
541 channel, GluCl<sup>41</sup>.

542 To compute the motor impact score of a given FeCO neuron onto a motor module (**Figure 3**), we  
543 summed together the calculated impact scores of direct, monosynaptic connections, disynaptic connections,  
544 and trisynaptic connections between the FeCO neuron and all MNs within a module. The impact score of  
545 monosynaptic connections between an FeCO neuron and a motor module is as described above but summed  
546 across all MNs within a module. We assume that FeCO input to MNs would be cholinergic, and thus  
547 excitatory.

548 For the impact score of a disynaptic connection, we first found all neurons with an identified  
549 hemilineage that were postsynaptic to the FeCO neuron and presynaptic to the MNs within the relevant  
550 module. We then multiplied the monosynaptic impact score from the FeCO neuron onto one of these  
551 postFeCO/preMN neurons by the impact score of the postFeCO/preMN neuron onto the MNs within a  
552 module. If the postFeCO/preMN neuron was identified as cholinergic, then this disynaptic impact score  
553 was considered to be excitatory/positive, and if it was identified as GABAergic or glutamatergic, then it  
554 was considered to be inhibitory/negative. We then summed together all disynaptic impact scores from the  
555 FeCO neuron to the MNs of a module.

556 For the impact score of a trisynaptic connection, we first found all neurons with an identified  
557 hemilineage that were postsynaptic to the FeCO neuron (postFeCOs), all neurons with an identified  
558 hemilineage that were presynaptic to the MNs within the relevant module (preMNs), and then only included  
559 postFeCO neurons that were presynaptic to a preMN neuron, and preMN neurons that were postsynaptic to  
560 a postFeCO neuron. We then multiplied the monosynaptic impact score from the FeCO neuron onto a  
561 postFeCO neuron by the impact score of the postFeCO neuron onto a preMN neuron, and this was  
562 multiplied by the impact score of the preMN neuron onto the MNs within a module. If both the postFeCO  
563 and preMN neurons were excitatory or both inhibitory, then this trisynaptic impact score was positive. If  
564 one neuron was inhibitory and one was excitatory, then this trisynaptic impact score was negative. We then  
565 summed together all trisynaptic impact scores from the FeCO neuron to the MNs of a module.

566

### 567 **Preference score**

568 To compute the preference score for a motor module (**Figure 3**), we summed the number of synapses onto  
569 each MN within a module (as defined by Lesser et al., 2023) and divided by the total synapses onto all  
570 MNs. To compute the sensory subtype preference score for a FeCO subtype (**Figure 3**), we summed the



571 number of synapses received from all FeCO neurons of a given subtype and divided by the total synapses  
572 received from all FeCO neurons.

573

### 574 **Circuit analysis in the FAFB/FlyWire connectome**

575 To study connectivity in the brain, we used the Full Adult Fly Brain connectome (FAFB; (Zheng et al.,  
576 2018) reconstructed and proofread by the FlyWire community (Dorkenwald et al., 2023a; Schlegel et al.,  
577 2023; Zheng). All data are from public release version 630.

578

### 579 **Identification of ascending neurons in FAFB/FlyWire connectome**

580 First, we manually screened through the repository of Gen1 MCFO images on FlyLight<sup>80</sup> for candidate  
581 images of VNCs that exhibit hallmark expression of the ascending club axons, ascending 8B interneurons,  
582 and ascending 10B interneurons in the VNC. To identify the anatomy of the ascending projections in the  
583 brain, we matched the ascending axons and interneurons in the VNC to the corresponding images in the  
584 brain. Next, we matched the anatomy of the ascending projections in the brain based on the light-level  
585 images to the FAFB dataset using flywire.ai<sup>82</sup> and the Codex platform<sup>83</sup>. Specifically, we queried neurons  
586 classified as ascending and cholinergic<sup>84,85</sup>, then matched candidates to the light-level images of the target  
587 neurons. See Supplemental **Table 3** for links to view the ascending neurons in Neuroglancer<sup>77</sup>.

588

### 589 **Software and data availability**

590 Data presented in the paper was analyzed from the CAVE materialization v604 timestamp  
591 1684915801.222989. Annotated connectivity matrices (**Figure 2**) will be available as python Pandas data  
592 frames (<https://pandas.pydata.org/>) at the git-hub repository: [https://github.com/sagrawal/Lee\\_2024](https://github.com/sagrawal/Lee_2024). Also  
593 available at the repository are scripts to recreate the analyses and figures in the paper, as well as scripts to  
594 recreate the connectivity matrices for users authorized to interact with the CAVEclient. Links to public  
595 segmentations are available throughout the text, as well as in a document at the git-hub repository. All  
596 analysis was performed in Python 3.9 using custom code, making extensive use of CAVEclient  
597 (<https://github.com/seung-lab/CAVEclient>) and CloudVolume to interact with data infrastructure, and  
598 libraries Matplotlib, Numpy, Pandas, Scikit-learn, Scipy, stats-models and VTK for general computation,  
599 machine learning and data visualization. Additional code is available at  
600 [https://github.com/htem/FANC\\_auto\\_recon](https://github.com/htem/FANC_auto_recon), providing additional tutorials, code and documentation for  
601 interacting with FANC.

602

- 604 1. O'Connor, D. H., Krubitzer, L. & Bensmaia, S. Of mice and monkeys: Somatosensory processing in two  
605 prominent animal models. *Prog. Neurobiol.* **201**, 102008 (2021).
- 606 2. Tuthill, J. C. & Wilson, R. I. Mechanosensation and Adaptive Motor Control in Insects. *Curr. Biol.* **26**, R1022–  
607 R1038 (2016).
- 608 3. Turecek, J. & Ginty, D. D. Coding of self and environment by Pacinian neurons in freely moving animals.  
609 2023.09.11.557225 Preprint at <https://doi.org/10.1101/2023.09.11.557225> (2023).
- 610 4. Reschechtko, S. & Pruszynski, J. A. Stretch reflexes. *Curr. Biol. CB* **30**, R1025–R1030 (2020).
- 611 5. Abaira, V. E. & Ginty, D. D. The Sensory Neurons of Touch. *Neuron* **79**, 618–639 (2013).
- 612 6. Macefield, V. G. The roles of mechanoreceptors in muscle and skin in human proprioception. *Curr. Opin.*  
613 *Physiol.* **21**, 48–56 (2021).
- 614 7. Dorkenwald, S. *et al.* Neuronal wiring diagram of an adult brain. *bioRxiv* 2023.06.27.546656 (2023)  
615 doi:10.1101/2023.06.27.546656.
- 616 8. Phelps, J. S. *et al.* Reconstruction of motor control circuits in adult *Drosophila* using automated transmission  
617 electron microscopy. *Cell* **184**, 759-774.e18 (2021).
- 618 9. Takemura, S. *et al.* A Connectome of the Male *Drosophila* Ventral Nerve Cord. 2023.06.05.543757 Preprint at  
619 <https://doi.org/10.1101/2023.06.05.543757> (2023).
- 620 10. Winding, M. *et al.* The connectome of an insect brain. *Science* **379**, eadd9330 (2023).
- 621 11. Zheng, Z. *et al.* A Complete Electron Microscopy Volume of the Brain of Adult *Drosophila melanogaster*. *Cell*  
622 **174**, 730-743.e22 (2018).
- 623 12. Hampel, S. *et al.* Distinct subpopulations of mechanosensory chordotonal organ neurons elicit grooming of the  
624 fruit fly antennae. *eLife* **9**, e59976 (2020).
- 625 13. Kim, H. *et al.* Wiring patterns from auditory sensory neurons to the escape and song-relay pathways in fruit  
626 flies. *J. Comp. Neurol.* **528**, 2068–2098 (2020).
- 627 15. Mamiya, A., Gurung, P. & Tuthill, J. C. Neural coding of leg proprioception in *Drosophila*. *Neuron* **100**, 636–  
628 650 (2018).
- 629 16. Phillis, R., Statton, D., Caruccio, P. & Murphey, R. K. Mutations in the 8 kDa dynein light chain gene disrupt  
630 sensory axon projections in the *Drosophila* imaginal CNS. *Development* **122**, 2955–2963 (1996).
- 631 17. Smith, S. A. & Shepherd, D. Central afferent projections of proprioceptive sensory neurons in *Drosophila*  
632 revealed with the enhancer-trap technique. *J. Comp. Neurol.* **364**, 311–323 (1996).
- 633 18. Field, L. H. & Matheson, T. Chordotonal Organs of Insects. in *Advances in Insect Physiology* (ed. Evans, P.  
634 D.) vol. 27 1–228 (Academic Press, 1998).
- 635 19. Mamiya, A. *et al.* Biomechanical origins of proprioceptor feature selectivity and topographic maps in the  
636 *Drosophila leg*. *Neuron* **111**, 3230-3243.e14 (2023).
- 637 20. Eberhard, M. J. B. *et al.* Structure and sensory physiology of the leg scolopidial organs in Mantophasmatodea  
638 and their role in vibrational communication. *Arthropod Struct. Dev.* **39**, 230–241 (2010).
- 639 21. Field, L. H. & Pflüger, H.-J. The femoral chordotonal organ: A bifunctional orthopteran (*Locusta migratoria*)  
640 sense organ? *Comp. Biochem. Physiol. A Physiol.* **93**, 729–743 (1989).
- 641 22. McKelvey, E. G. Z. *et al.* *Drosophila* females receive male substrate-borne signals through specific leg neurons  
642 during courtship. *Curr. Biol.* **31**, 3894-3904.e5 (2021).
- 643 23. Takanashi, T., Fukaya, M., Nakamuta, K., Skals, N. & Nishino, H. Substrate vibrations mediate behavioral  
644 responses via femoral chordotonal organs in a cerambycid beetle. *Zool. Lett.* **2**, 18 (2016).
- 645 24. Agrawal, S. *et al.* Central processing of leg proprioception in *Drosophila*. *eLife* **9**, e60299 (2020).

- 646 25. Chen, C. *et al.* Functional architecture of neural circuits for leg proprioception in *Drosophila*. *Curr Biol* **31**,  
647 5163-5175.e7 (2021).
- 648 26. Azevedo, A. *et al.* Tools for comprehensive reconstruction and analysis of *Drosophila* motor circuits. (2022)  
649 doi:10.1101/2022.12.15.520299.
- 650 27. Lesser, E. *et al.* Synaptic architecture of leg and wing motor control networks in *Drosophila*. *bioRxiv*  
651 2023.05.30.542725 (2023) doi:10.1101/2023.05.30.542725.
- 652 28. Azevedo, A. W. *et al.* A size principle for recruitment of *Drosophila* leg motor neurons. *Elife* **9**, e56754 (2020).
- 653 29. Dallmann, C. J., Agrawal, S., Cook, A., Brunton, B. W. & Tuthill, J. C. Presynaptic inhibition selectively  
654 suppresses leg proprioception in behaving *Drosophila*. *bioRxiv* 2023.10.20.563322 (2023).
- 655 30. Scheffer, L. K. *et al.* A connectome and analysis of the adult *Drosophila* central brain. *eLife* **9**, e57443 (2020).
- 656 31. Schlegel, P. *et al.* Whole-brain annotation and multi-connectome cell typing quantifies circuit stereotypy in  
657 *Drosophila*. 2023.06.27.546055 Preprint at <https://doi.org/10.1101/2023.06.27.546055> (2023).
- 658 32. Truman, J. W., Moats, W., Altman, J., Marin, E. C. & Williams, D. W. Role of Notch signaling in establishing  
659 the hemilineages of secondary neurons in *Drosophila melanogaster*. *Development* **137**, 53–61 (2010).
- 660 33. Lacin, H. *et al.* Neurotransmitter identity is acquired in a lineage-restricted manner in the *Drosophila* CNS.  
661 *eLife* **8**, e43701 (2019).
- 662 34. Allen, A. M. *et al.* A single-cell transcriptomic atlas of the adult *Drosophila* ventral nerve cord. *bioRxiv*  
663 2019.12.20.883884 (2019) doi:10.1101/2019.12.20.883884.
- 664 35. Lacin, H. & Truman, J. W. Lineage mapping identifies molecular and architectural similarities between the  
665 larval and adult *Drosophila* central nervous system. *eLife* **5**, e13399 (2016).
- 666 36. Harris, R. M., Pfeiffer, B. D., Rubin, G. M. & Truman, J. W. Neuron hemilineages provide the functional  
667 ground plan for the *Drosophila* ventral nervous system. *eLife* **4**, e04493 (2015).
- 668 37. Mark, B. *et al.* A developmental framework linking neurogenesis and circuit formation in the *Drosophila* CNS.  
669 *eLife* **10**, e67510 (2021).
- 670 38. Li, H. *et al.* Fly Cell Atlas: A single-nucleus transcriptomic atlas of the adult fruit fly. *Science* **375**, eabk2432  
671 (2022).
- 672 39. Gowda, S. B. M. *et al.* GABAergic inhibition of leg motoneurons is required for normal walking behavior in  
673 freely moving *Drosophila*. *Proc. Natl. Acad. Sci.* **115**, E2115–E2124 (2018).
- 674 40. Lees, K. *et al.* Actions of agonists, fipronil and ivermectin on the predominant in vivo splice and edit variant  
675 (RDLbd, I/V) of the *Drosophila* GABA receptor expressed in *Xenopus laevis* oocytes. *PloS One* **9**, e97468  
676 (2014).
- 677 41. Liu, W. W. & Wilson, R. I. Glutamate is an inhibitory neurotransmitter in the *Drosophila* olfactory system.  
678 *Proc. Natl. Acad. Sci. U. S. A.* **110**, 10294–10299 (2013).
- 679 42. Zill, S. N., Chaudhry, S., Büschges, A. & Schmitz, J. Force feedback reinforces muscle synergies in insect legs.  
680 *Arthropod Struct. Dev.* **44**, 541–553 (2015).
- 681 43. King, D. G. & Wyman, R. J. Anatomy of the giant fibre pathway in *Drosophila*. I. Three thoracic components  
682 of the pathway. *J. Neurocytol.* **9**, 753–770 (1980).
- 683 44. Tanouye, M. A. & Wyman, R. J. Motor outputs of giant nerve fiber in *Drosophila*. *J. Neurophysiol.* **44**, 405–  
684 421 (1980).
- 685 45. Patella, P. & Wilson, R. I. Functional Maps of Mechanosensory Features in the *Drosophila* Brain. *Curr. Biol.*  
686 *CB* **28**, 1189-1203.e5 (2018).
- 687 46. Ishikawa, Y., Okamoto, N., Nakamura, M., Kim, H. & Kamikouchi, A. Anatomic and Physiologic  
688 Heterogeneity of Subgroup-A Auditory Sensory Neurons in Fruit Flies. *Front. Neural Circuits* **11**, 46 (2017).

- 689 47. Yorozu, S. *et al.* Distinct sensory representations of wind and near-field sound in the *Drosophila* brain. *Nature*  
690 **458**, 201–205 (2009).
- 691 48. Matsuo, E. *et al.* Organization of projection neurons and local neurons of the primary auditory center in the  
692 fruit fly *Drosophila melanogaster*. *J. Comp. Neurol.* **524**, 1099–1164 (2016).
- 693 49. Baker, C. A. *et al.* Neural network organization for courtship-song feature detection in *Drosophila*. *Curr. Biol.*  
694 *CB* **32**, 3317–3333.e7 (2022).
- 695 50. Burrows, M. & Horridge, G. A. The organization of inputs to motoneurons of the locust metathoracic leg.  
696 *Philos. Trans. R. Soc. Lond. B. Biol. Sci.* **269**, 49–94 (1974).
- 697 51. Field, L. H. & Rind, F. C. A single insect chordotonal organ mediates inter- and intra-segmental leg reflexes.  
698 *Comp. Biochem. Physiol. A Physiol.* **68**, 99–102 (1981).
- 699 52. Azim, E. & Seki, K. Gain control in the sensorimotor system. *Curr. Opin. Physiol.* **8**, 177–187 (2019).
- 700 53. Koch, S. C. *et al.* ROR $\beta$  Spinal Interneurons Gate Sensory Transmission during Locomotion to Secure a Fluid  
701 Walking Gait. *Neuron* **96**, 1419–1431.e5 (2017).
- 702 54. McComas, A. J. Hypothesis: Hughlings Jackson and presynaptic inhibition: is there a big picture? *J.*  
703 *Neurophysiol.* **116**, 41–50 (2016).
- 704 55. Chockley, A. S. *et al.* Subsets of leg proprioceptors influence leg kinematics but not interleg coordination in  
705 *Drosophila melanogaster* walking. *J. Exp. Biol.* **225**, jeb244245 (2022).
- 706 56. Delcomyn, F. Factors Regulating Insect Walking. *Annu. Rev. Entomol.* **30**, 239–256 (1985).
- 707 57. Pratt, B. G., Lee, S.-Y. J., Chou, G. M. & Tuthill, J. C. Miniature linear and split-belt treadmills reveal  
708 mechanisms of adaptive motor control in walking *Drosophila*. 2024.02.23.581656 Preprint at  
709 <https://doi.org/10.1101/2024.02.23.581656> (2024).
- 710 58. Laurent, G. & Burrows, M. Intersegmental interneurons can control the gain of reflexes in adjacent segments of  
711 the locust by their action on nonspiking local interneurons. *J. Neurosci. Off. J. Soc. Neurosci.* **9**, 3030–3039  
712 (1989).
- 713 59. Chen, C.-L. *et al.* Ascending neurons convey behavioral state to integrative sensory and action selection brain  
714 regions. *Nat. Neurosci.* **26**, 682–695 (2023).
- 715 60. Cruz, T. L. & Chiappe, M. E. Multilevel visuomotor control of locomotion in *Drosophila*. *Curr. Opin.*  
716 *Neurobiol.* **82**, 102774 (2023).
- 717 61. Fujiwara, T., Brotas, M. & Chiappe, M. E. Walking strides direct rapid and flexible recruitment of visual  
718 circuits for course control in *Drosophila*. *Neuron* **110**, 2124–2138.e8 (2022).
- 719 62. Pfeiffer, K. & Homberg, U. Organization and functional roles of the central complex in the insect brain. *Annu.*  
720 *Rev. Entomol.* **59**, 165–184 (2014).
- 721 64. Hill, P. S. M. & Wessel, A. Biotremology. *Curr. Biol.* **26**, R187–R191 (2016).
- 722 65. Huey, E. L. *et al.* The auditory midbrain mediates tactile vibration sensing. *bioRxiv* 2024.03.08.584077 (2024)  
723 doi:10.1101/2024.03.08.584077.
- 724 66. Virant-Doberlet, M., Stritih-Peljhan, N., Žunič-Kosi, A. & Polajnar, J. Functional Diversity of Vibrational  
725 Signaling Systems in Insects. *Annu. Rev. Entomol.* **68**, 191–210 (2023).
- 726 67. Burke, W. An Organ for Proprioception and Vibration Sense in *Carcinus Maenas*. *J. Exp. Biol.* **31**, 127–138  
727 (1954).
- 728 68. Cohen, M. J. The crustacean myochordotonal organ as a proprioceptive system. *Comp. Biochem. Physiol.* **8**,  
729 223–243 (1963).
- 730 69. Salmon, M., Horch, K. & Hyatt, G. Barth’s myochordotonal organ as a receptor for auditory and vibrational  
731 stimuli in fiddler crabs (*Uca pugilator* and *U. minax*). *Mar. Freshw. Behav. Phy* **4**, 187–194 (1977).
- 732 70. Ewing, A. W. & Bennet-Clark, H. C. The Courtship Songs of *Drosophila*. *Behaviour* **31**, 288–301 (1968).

- 733 71. Kamikouchi, A. *et al.* The neural basis of *Drosophila* gravity-sensing and hearing. *Nature* **458**, 165–171  
734 (2009).
- 735 72. Murthy, M. Unraveling the auditory system of *Drosophila*. *Curr. Opin. Neurobiol.* **20**, 281–287 (2010).
- 736 73. Shorey, H. H. Nature of the Sound Produced by *Drosophila melanogaster* during Courtship. *Science* **137**, 677–  
737 678 (1962).
- 738 74. Fabre, C. C. G. *et al.* Substrate-Borne Vibratory Communication during Courtship in *Drosophila*  
739 *melanogaster*. *Curr. Biol.* **22**, 2180–2185 (2012).
- 740 75. Gebehart, C., Hooper, S. L. & Büschges, A. Non-linear multimodal integration in a distributed premotor  
741 network controls proprioceptive reflex gain in the insect leg. *Curr. Biol. CB* **32**, 3847-3854.e3 (2022).
- 742 76. Gebehart, C. & Büschges, A. The processing of proprioceptive signals in distributed networks: insights from  
743 insect motor control. *J. Exp. Biol.* **227**, jeb246182 (2024).
- 744 77. Maitin-Shepard, J. *et al.* google/neuroglancer: Zenodo <https://doi.org/10.5281/zenodo.5573294> (2021).
- 745 78. Dorkenwald, S. *et al.* CAVE: Connectome Annotation Versioning Engine. *bioRxiv* 2023.07.26.550598 (2023)  
746 doi:10.1101/2023.07.26.550598.
- 747 79. Marin, E. C. *et al.* Systematic annotation of a complete adult male *Drosophila* nerve cord connectome reveals  
748 principles of functional organisation. *bioRxiv* 2023.06.05.543407 (2023) doi:10.1101/2023.06.05.543407.
- 749 80. Meissner, G. W. *et al.* A searchable image resource of *Drosophila* GAL4 driver expression patterns with single  
750 neuron resolution. *eLife* **12**, e80660 (2023).
- 751 81. Buhmann, J. *et al.* Automatic detection of synaptic partners in a whole-brain *Drosophila* electron microscopy  
752 data set. *Nat. Methods* **18**, 771–774 (2021).
- 753 82. Dorkenwald, S. *et al.* FlyWire: online community for whole-brain connectomics. *Nat. Methods* **19**, 119–128  
754 (2022).
- 755 83. Matsliah, A. *et al.* Neuronal “parts list” and wiring diagram for a visual system. *bioRxiv* 2023.10.12.562119  
756 (2023) doi:10.1101/2023.10.12.562119.
- 757 84. Eckstein, N. *et al.* Neurotransmitter Classification from Electron Microscopy Images at Synaptic Sites in  
758 *Drosophila Melanogaster*. 2020.06.12.148775 Preprint at <https://doi.org/10.1101/2020.06.12.148775> (2023).
- 759 85. Heinrich, L., Funke, J., Pape, C., Nunez-Iglesias, J. & Saalfeld, S. Synaptic Cleft Segmentation in Non-  
760 isotropic Volume Electron Microscopy of the Complete *Drosophila* Brain. in *Medical Image Computing and*  
761 *Computer Assisted Intervention – MICCAI 2018* (eds. Frangi, A. F., Schnabel, J. A., Davatzikos, C., Alberola-  
762 López, C. & Fichtinger, G.) 317–325 (Springer International Publishing, Cham, 2018). doi:10.1007/978-3-030-  
763 00934-2\_36.
- 764